Australasian Physical & Engineering Sciences in Medicine (2019) 42:427–441
https://doi.org/10.1007/s13246-019-00735-8

SCIENTIFIC PAPER

Influence of normalization and color features on super-pixel classification: application to cytological image segmentation

Mohammed El Amine Bechar[1,2] · Nesma Settouti[2] · Mostafa El Habib Daho[2] · Mouloud Adel[1] · Mohammed Amine Chikh[2]

Received: 1 June 2018 / Accepted: 15 February 2019 / Published online: 4 March 2019

Abstract
Super-pixel feature extraction is a key problem to get an acceptable performance in color super-pixel classification. Given a color feature extraction problem, it is necessary to know which is the best approach to solve this problem. In the current work, we're interested in the challenge of nucleus and cytoplasm automatic recognition in the cytological image. We propose an automatic process for white blood cells (WBC) segmentation using super-pixel classification. The process is divided into five steps. In first step, the color normalization is calculated. The super-pixels generation by Simple Linear Iterative Clustering algorithm is performed in the second step. In third step, the color property is used to achieve illumination invariance. In fourth step, color features are calculated on each super-pixel. Finally, supervised learning is realized to classify each super-pixel into nucleus and cytoplasm region. The present work rallied an exhaustive statistical evaluation of a very wide variety of the color super-pixel classification, with height normalization methods, four-color spaces and four feature extraction techniques. Normalization and color spaces slightly increase the average accuracy of super-pixel classification. Our experiments based to statistical comparison allow to conclude that comprehensive gray world normalized normalization is better than without normalization for super-pixel classification achieving the first positions in the Friedman ranking. RGB space is the best color spaces to be used in super-pixel feature extraction for nucleus and cytoplasm segmentation. For feature extraction, the learning methods work better on the first order statistics features for the automatic WBC segmentation.

Keywords Super-pixel classification · Image normalization · Color space · Feature extraction · Supervised classification · White blood cells

Introduction

One of the highlighted areas in hematology disease is the problem of White Blood Cells (WBC) automatic detection. WBC segmentation is the main step for reliable pattern recognition [19]. The cytological image segmentation uses the information from image (color, gray level or spatial) to identify the different anatomical structures in WBC which consist of nucleus and cytoplasm.

Several works have been carried out on the study of color information in the segmentation and classification of certain diseases and tumors. Irshad et al. [24] present a work that combines techniques that are most commonly used for nucleus segmentation in microscopic imaging (Hematoxylin-Eosin (H&E) and ImmunoHistoChemical (IHC) images). This study highlights the main trends of segmentation, feature extraction and classification of nucleus based on an exhaustive view of different techniques available in the literature.

Pursuant to [24, 25], the current trend is the application of artificial intelligence for automatic segmentation. Particularly, the integration of super-pixel techniques in the segmentation process, this has a potential in the color images segmentation.

Super-pixel classification is an area that has been studied extensively for segmentation applications. The super-pixel was introduced by Ren and Malik [37]. Its principle is to describe various groups of similar pixels in color or other properties of image. Super-pixel classification assigned a

✉ Mohammed El Amine Bechar
mohammed.bechar@fresnel.fr

[1] CNRS, Centrale Marseille, Aix Marseille Univ, Institut Fresnel UMR 7249, 13013 Marseille, France

[2] Biomedical Engineering Laboratory GBM, Tlemcen University, Tlemcen, Algeria

region class to each super-pixel of the image taking into account the set of known region classes, this can accelerate and improve the quality of segmentation.

The main steps used in the super-pixel classification process usually consist in: preprocessing of image, computing super-pixels, extracting features to transform each super-pixel into a feature vector, and finally classifying each feature vector to one of the available region classes.

The success of this process of segmentation lies in three main steps:

- First, an image preprocessing step.
- Next, an adapted feature extraction technique to the segmentation problem.
- At last, a good choice of the classifier, to generate a robust hypothesis for a reliable super-pixel classification.

In this context, Cernadas et al. [10] and González-Rufino et al. [19] present an exhaustive evaluation of different feature extraction techniques based on color and texture information. Cernadas et al. [10] studied the influence of color normalization on segmentation. González-Rufino et al. [19] presented a complete list of several feature extraction techniques for better recognition of the nucleus in histological image.

Indeed, color analysis, which uses chromatic properties to characterize an image, has attracted significant attention [12, 27]. The illumination represent an important parameter for producing relevant color information in the image acquisition. Therefore, illumination variation is a very important issue in feature extraction based on color information because it has a direct impact in segmentation results.

Given a super-pixel classification problem, it's essential to know which is the best approach to solve this problem making the minimal assumptions about the segmentation process conditions. The proposed solutions to achieve a good segmentation can be enclosed in five treatment: image normalization for achieving illumination invariance [27], super-pixel setting, pertinent choice of color space [3, 14, 31], best feature extraction methods and robust classification technique.

The integration of super-pixel in the segmentation process revealed a new research area in the automatic segmentation. In this article, we study several issues that have positive or negative affect on the quality of segmentation using the super-pixel classification process. We synthesize our inquiry in the following points:

- The effect of color normalization on segmentation results.
- The most suitable color space for color image segmentation.
- The super-pixel feature extraction study.

Super-pixel based classification for image segmentation has proven its effectiveness and its application value in various fields. In point of fact, several works have been made in super-pixel classification for automatic segmentation of medical imaging: IRM, scanner, retinal, microscopic, etc., ...with different contributions.

In order to detect glaucomas damage at early stages on 3D SD-OCT images; Xu et al. [45] proposed an algorithm uses self-size-adjusting super-pixel classification by boosting approach to quantitatively assess the 3D dataset in order to improve glaucoma detection.

Always on medical context, Magana-Tellez et al. [32] present an algorithm for the localization and quantification of cells in histological images named super-pixel classification for cell detection and counting (SPICE). The principle of this algorithm is to perform super-pixels pretreatment on the image, followed by a classification steps with two random forests. The first random forest determines if the super-pixel at its input contains any cells, the second provides the number of cells in the respective super-pixel.

Wu et al. [44] have developed a robust segmentation method for brain tumor MRI. Multi-modal MR images are segmented into super-pixels using the appropriate algorithm to alleviate the sampling issue and to improve the sample representativeness. Next, multi-level Gabor wavelet filters are applied to extract features from each super-pixel. From these extracted characteristics, the SVM model is trained and an affinity model for tumor is learned from the training data set. Thereafter, conditional random fields theory was practiced to segment the tumor in a maximum a posteriori fashion given the smoothness prior defined by the proposed affinity model. Finally, labeling noise was removed using "structural knowledge" such as the symmetrical and continuous characteristics of the tumor in a spatial domain.

Unlike previous super-pixel classification approaches, Borovec et al. [7] extend the classical segmentation pipeline by spatial regularization using Graph Cut to encourage spatial continuity. This segmentation schemes is applied on five real-world medical imaging. The results show an improvement over segmentations by Graph Cut at pixels, the super-texton and super-pixels.

By sweeping the state of the art of the domain, usually super-pixel based segmentation methods, includes three stages: first, compute pre-segmentation by a super-pixels method; second, extract super-pixel features; finally, use a classifier to assign labels to super-pixels and extend them to the whole image. The classification can be performed in a supervised [4, 8, 11, 35] unsupervised [17, 34, 44] and semi-supervised learning [5, 20].

In this paper, we only focus on the second step in the super-pixel segmentation pipeline, which is the most important. Previous work proved that super-pixels can perform better than pixel-level segmentation, with lower demands on

time and resources, also studies demonstrated that a more suitable classification scheme improves the segmentation results, but the fact remains that the feature extraction step is the most crucial and especially in super-pixel images. Therefore, we study a wide comparison of different combinations of normalizations, color spaces and color features extraction that have an impact on the segmentation quality. The principal objective of this work is to highlight the super-pixel feature extraction that have an influence on the quality of segmentation process.

The study present in this paper is organized as follows. In Sect. 2, we discuss the general concept of the segmentation process. In Sect. 3, we explain the materials and methods used in our proposed. In Sects. 4 and 5, we show results and discussion from exhaustive validation of our process. We end with discussion and conclusion in Sect. 6.

Segmentation by super-pixel classification

The present work aims to automatic *nucleus* and *cytoplasm* segmentation for white blood cells recognition. In our proposal, the segmentation is achieved by supervised super-pixel classification, whose intervention of an area expert is essential in the identification of the *nucleus*, *cytoplasm*, *Red Blood Cell* and *background* super-pixels. The proposed segmentation scheme is illustrated in Fig. 1.

Image pretreatment aims to improve the image quality in order to facilitate the segmentation process by improving the similarity between pixels in the same region, and the dissimilarity between different regions. There is different pretreatment technique such as: normalization, enhancement, filtering, compression. We begin our treatment with data normalization as a pretreatment, and that represents an important study in our work.

A super-pixel provides an important primitive quality that will be exploited to compute local features. Another advantage of super-pixels is that they reduce redundant information in image [38] and thus significantly reduce the complexity of subsequent image processing tasks. They have become important tools for different applications such as depth estimation [22], image segmentation [21, 29], skeletonization [28], and object localization [18].

The second step in our proposed method is the application of the simple linear iterative clustering algorithm (*SLIC*) [2] that generates a set of super-pixels in the image, a super-pixel is composed of a group of pixels sharing a similarity according to the color. Achanta et al. [2] proposed a 5-Dimensional distance measure to calculate super-pixels. Lab color space and x; y pixel coordinates are combined, the new distance D_s (Eq. 1) considers super-pixel size to enforce color similarity and pixel proximity:

$$\begin{aligned} d_{lab} &= \sqrt{(l_k - l_i)^2 + (a_k - a_i)^2 + (b_k - b_i)^2}, \\ d_{xy} &= \sqrt{(x_k - x_i)^2 + (y_k - y_i)^2}, \\ D_s &= d_{lab} + \frac{m}{S} d_{xy}, \end{aligned} \tag{1}$$

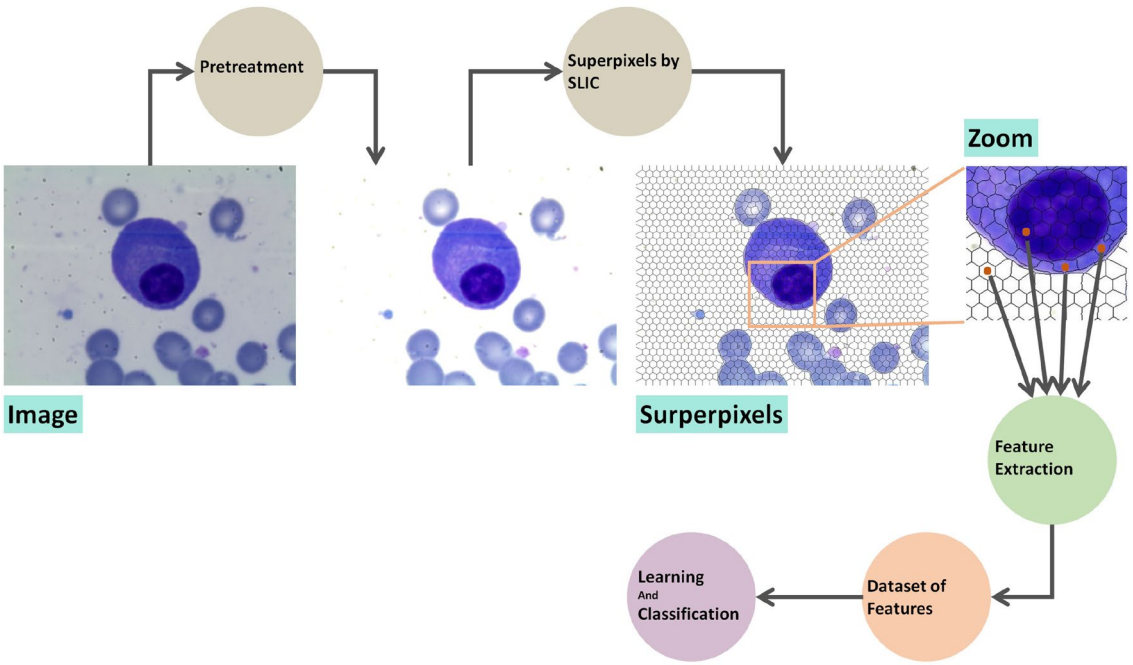

Fig. 1 Segmentation scheme by super-pixel classification

where d_{Lab} is the lab distance, d_{xy} is the plane distance normalized by the grid interval S and the variable m is introduced to control the compactness of a super-pixel. This value can be in the range [1–20].

The feature extraction is an important step in this segmentation process, it is aimed at presenting each super-pixel as a features vector (FV). Mathematical calculations will be applied to each super-pixel based on the color information. In this process, segmentation is done in the last step by preparing a supervised classifier to classify the super-pixels of the image. Sections 3 and 4 provide more details on the proposed approach.

Material and methods

The proposed process include the image normalization to standardize the color information, and the color space transformation to vary the color component.

Image normalization

The necessary tools for designing a cytological image acquisition environment are: a specific camera, a microscope, and software. RGB color space is the fundamental format used in most color image acquisition environments corresponding to Red, Green and Blue colors respectively. In color images, the information on the structure of an observed region is essentially affected by the color information. This information itself changes considerably depending on several factors such as the type of acquisition sensor and the lighting conditions [27].

Some studies use the normalization process as a preprocessing to produce a more uniform image. Cernadas et al. [10] demonstrated the significant improvement of image analysis using color normalization. The normalization of an image is a step that consists in producing an invariant description event if the lighting conditions change. The normalization processing is considered as an important step before texture features computing in order to minimize the effect of intensity variations [26, 42, 43]. The normalization is also applied to color images before other processing [27, 39]. Different mathematical operations are applied in color normalization [15] to modify the color intensity of each pixel to reduce out all variables that are dependent on illumination. In this study we use the invariant color normalizations as studied by Cernadas et al. [10]: Chroma, GWN, CGWN, HEQ, CLAHE, RGBcb, RGBib, MV and Lmax. Moreover, the WN image is noted as an image without normalization.

Chroma (chromaticity) is a normalization technique that is often used by computer vision system, it is obtained using the chromaticity of the three spaces (Red, Green and Blue) independently of the observed light intensity. The Chroma representation $R'G'B'$ is derived from a RGB image by:

$$(R', G', B') = \left(\frac{R}{R+G+B}, \frac{G}{R+G+B}, \frac{B}{R+G+B}\right). \quad (2)$$

GWN (grey world normalization) is a basic normalization that assumes any changes in the illumination spectrum can be modeled by three constant factors (R_{avg}, G_{avg} and B_{avg}) applied to Red, Green and Blue color spaces.

$$R' = \frac{R}{R_{avg}}, G' = \frac{G}{G_{avg}}, B' = \frac{B}{B_{avg}}, \quad (3)$$

where the triplet (R_{avg}, G_{avg} and B_{avg}) denotes the mean of R,G and B spaces.

CGWN (comprehensive gray world normalized) is a normalization technique that combines the *CHROMA* and *GWN* techniques [16] by using the local information of each R, G and B spaces and the global chromaticity information. This normalization is computed iteratively and successively by applying the Eqs. 2 and 3, this converges to a normalized representation depending on color intensity and color luminance.

HEQ (histogram equalization) is an image processing technique that enhances the overall contrast in the image. This technique is originally developed for a gray-scale images. A mathematical transformation is applied to have a uniform histogram, which maximizes the entropy and image information content. To improve the image quality and eliminate the lighting effects produced by the acquisition, Finlayson et al [16] used this transformation for each color space in an image as a normalized representation.

CLAHE (contrast limited adaptive histogram equalization) CLAHE is an improved extension of histogram equalization technique (HEQ), primarily developed for medical imaging and has proven to be effective in enhancing low contrast images, which also attempts to solve its problems of noise amplification [46]. The CLAHE was originally developed for grayscale images and it can be extended to color images by applying this technique to Red, Green and Blue spaces. The result of CLAHE is considered as normalized and improved image according to contrast and entropy information.

RGBcb (RGB color balance) is an algorithm used to correct under-exposed images or images taken in artificial/special natural lights. This algorithm assumes that the high values of Red, Green and Blue observed in the color image must correspond to white, and the low values to obscurity. The objective of RGBcb is to spread as it possible the intensity values of the red, green and blue spaces, so that they occupy the maximum possible Rang [0, 255]. We use the implementation provided by Lumire et al. [30].

MV (mean variance) A normalized image is characterized by a zero Mean and unit Variance, this method is applied to gray-scale image. Cernadas et al [10] proposed applying the zero mean and unit variance *MV* to each color space in the RGB image.

$\boldsymbol{L}_{max}$ is a simple normalization procedure applied to each space in color image to minimize the lighting effects. Let $L_{i,max}, i \in \{r, g, b\}$ be the maximum value of each space i, and each pixel of the image is controlled by this maximum luminance as follows:

$$(R', G', B') = \left(\frac{R}{L_{r,max}}, \frac{G}{L_{g,max}}, \frac{B}{L_{b,max}}\right). \quad (4)$$

Color space

The R, G and B are the most exploited spaces in color image processing because it's the fundamental format used in acquisition devices. Thus, good segmentation and classification results can be obtained using the RGB space under controlled illumination conditions. Furthermore, different researchers investigate the effect of using different color space for color classification [14, 36]. An open question concerns the best performing color space, the good choice may bring considerable improvements in image classification [15]. Four main families [40] can be grouped into most classical color spaces as represent in Table 1.

An important issue that has been addressed by many researchers, it's to find the most suitable color space for color image segmentation. Vandenbroucke et al. [41] presented a summary of some work that offers a selective list of better color space. The synthesis of they work can agree with four relevant spaces, specifically RGB, Lab, HSV and I1I2I3. The same conclusion was achieved by Cernadas et al. [10], which focused only on four color spaces of each families. In this work, we choose one color space of each family exactly as was studied by Cernadas et al. [10]:

- The primary color spaces: *RGB*.
- The luminance –chrominance color spaces: *Lab*.
- The perceptual color color spaces: *HSV*.
- The independent axis color spaces: *I1I2I3*.

Table 1 Colors spaces [40]

Familie	Color spaces
Primary color	(R, G, B), (r, g, b)
	(X, Y, Z), (x, y, z)
Luminance–chrominance color	$(A, C1, C2)$, (bw, rg, by)
	(Y', I', Q'), (Y', U', V')
	(L, a, b), (L, u, v)
	(Y, Ch_1, Ch_2)
	(Y, x, y), $(I1, r, g)$
Perceptual color	$(I1, S1, H1)$, $(I1, S2, H1)$
	(H, S, V), (H, S, L)
	$(I6, S5, H1)$, (L, S_{UV}, H_{UV})
	(A, C_{C1C2}, h_{C1C2}), (bw, C_{rgby}, h_{rgby})
	(Y', C'_{IQ}, h'_{IQ}), (Y', C'_{UV}, h'_{UV})
	(L', C_{ab}, h_{ab}), (L', C'_{UV}, h_{UV})
	$(L, C_{Ch_1Ch_2}, h_{Ch_1Ch_2})$
	$(I1, C_{I2I3}, h_{I2I3})$
Independent color axis	$(I1, I2, I3)$

Super-pixel feature extraction

The numerical representation of a visual characteristic such as color, texture or shape is the most important step in an automatic recognition process, this is recognized by the feature extraction process. Several feature extraction methods are proposed in the literature that can be exploited in many applications. However, the choice of effective characteristics to solve a specific problem has become an important issue to which we are interested. Our work is essentially based on the study of the color effect in the super-pixel classification for white blood cells segmentation. Once the image is subdivided into super-pixels (*SP*), each one can be characterized by 3 color informations of each space $\{S_1, S_2, S_3\}$ and each super-pixel contains the n intensity values I (Fig. 2) (Example: In the RGB space, each super-pixel will be characterized by I_n intensity on each spaces $S_1 = R$, $S_2 = G$ and $S_3 = B$). Pure color feature techniques are used to converse the color information into a features vector (*FV*) (Fig. 2) which will be used in a classification process.

Color mean (CM)

It is one of the most basic feature extraction existing in the literature, the features vector (*FV*) simply includes 3 parameters $\{\mu^{S_1}, \mu^{S_2}, \mu^{S_3}\}$ extracted from each color space $S_j \in \{S_1, S_2, S_3\}$ by calculating the mean of the intensities in (Eq. 5):

$$\mu^{S_j} = \frac{1}{n}\sum_{i=1}^{n} I_i, \quad j = 1, 2, 3. \quad (5)$$

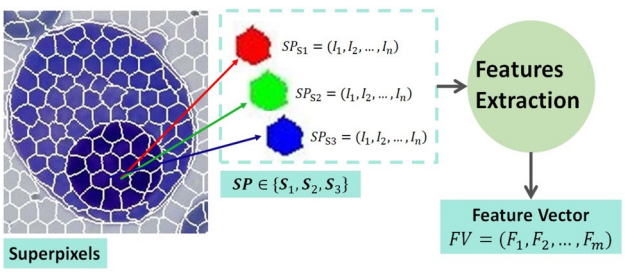

Fig. 2 Super-pixel feature extraction

First-order statistics (FOS)

The FOS features are statistical measures that can be applied for each super-pixel, to provide information about the distribution of gray levels in each color space $S_j \in \{S_1, S_2, S_3\}$. They are the simplest measures to characterize each super-pixel in image, but considered effective. The feature vector FOS includes 5 statistical measures on each color space (15 features in total). The features computed are [19]: mean level (μ^{S_j}), variance (σ^{S_j}), third ($m_3^{S_j}$) and four ($m_4^{S_j}$) statistical moments, and entropy (H^{S_j}):

$$\mu^{S_j} = \frac{1}{n}\sum_{i=1}^{n} I_i, \quad j = 1,2,3, \tag{6}$$

$$\sigma^{S_j} = \sqrt{\sum_{i\in SP}(i-\mu^{S_j})^2 I_i}, \quad j = 1,2,3, \tag{7}$$

$$m_3^{S_j} = \sum_{i\in SP}(i-\mu^{S_j})^3 I_i, \quad j = 1,2,3, \tag{8}$$

$$m_4^{S_j} = \sum_{i\in SP}(i-\mu^{S_j})^4 I_i, \quad j = 1,2,3, \tag{9}$$

$$H^{S_j} = -\sum_{i\in SP} I_i log(I_i), \quad j = 1,2,3. \tag{10}$$

Contrast

Contrast produces useful information between a given region and its neighborhood depending on the intensity value. Low contrast indicates strong similarity with neighboring super-pixels. Domingo Mery [33] set the contrast as follows:

$$C_1 = \frac{\mu_{SP_i} - \mu_{SP_j}}{\mu_{SP_j}}, \quad C_2 = \frac{\mu_{SP_i} - \mu_{SP_j}}{\mu_{SP_i} + \mu_{SP_j}}, \quad C_3 = ln(\mu_{SP_i}/\mu_{SP_j}), \tag{11}$$

where μ_{SP_i} and μ_{SP_j} indicate the mean value of gray level in the super-pixel SP_i and in the neighboring super-pixel SP_j respectively.

Hu Moments with intensity

Moments and their invariants have been extensively analyzed in many pattern recognition applications to characterize a region in the image, we cite: the geometrical moments [23], rotation moments [9] and the complex moments [1].

The invariant moments were introduced by Hu [23], he defined 6 absolute and an oblique orthogonal invariant, these measures are based on algebraic invariants that are independent of position, size, orientation, and parallel projection. The Hu moments are defined by:

$$m_{rs} = \sum_{i,j} i^r j^s \quad avec \quad r,s \in N, \tag{12}$$

where i and j denote the coordinates in an image and $r, s \in N$ are the moment order.

Domingo Mery [33] considered the gray level information in Hu's moments as a relevant feature extraction in automatic recognition. Hu moments with intensity are calculated as follows:

$$m_{rs} = \sum_{i,j} i^r j^s I(i,j), \tag{13}$$

where I is the intensity of the gray level.

Results

The success of the super-pixel classification lies in the efficiency of the data preprocessing step, so it became fundamental to study the feature extraction phase in which we are trying to answer the questions related to the normalization, color space and feature extraction technique.

The treatments mentioned allow an exhaustive study on the quality of the measured characteristics, where the reliability of feature extraction is essential in the quality of the super-pixel classification.

Database

The cytological images database was collected from real images acquired within the hemobiology department (CHU Tlemcen) [6], on MGG (May Grunwald Giemsa) staining slides. The LEICA environment (camera and microscope) allows obtaining RGB color images within 768 × 1024 size. 87 cytological images with ground truth are used for this experimental study. For our experiments, we selected 15% of the database (13 images) to prepare a learning base. The expert hematologist will intervene in the labeling these thirteen images by a selection of super-pixel of each region of interest (ROI), thus allowing a better perception of the *nucleus, cytoplasm, red cell* and *background* regions.

Experiments

An experimental plan is proposed in order to better answer the question "what affect the quality of segmentation using the super-pixel classification process?", the Fig. 3

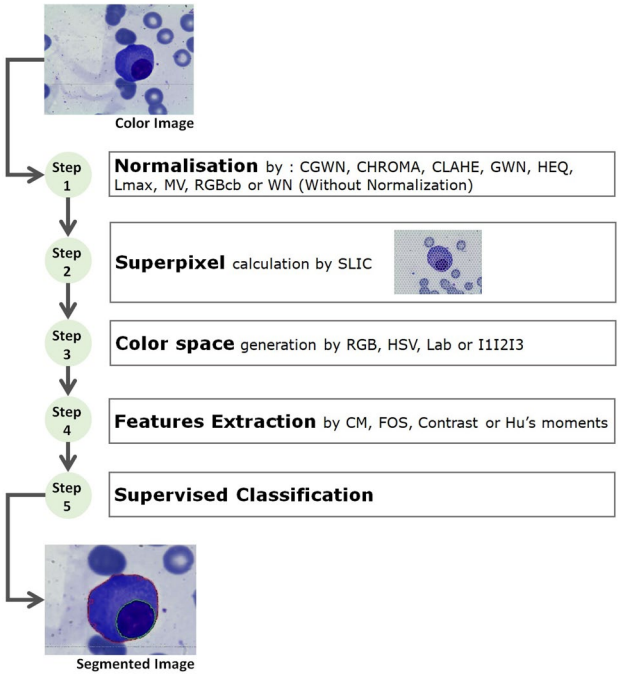

Fig. 3 Experimental plan

summarizes the steps of our experimental plan. The applied treatments start from *Step 1* to *Step 5*.

- *Step 1: Normalization* aims to study the influence of color normalization using different normalization techniques; this allows us to compare the results with respect to segmentation without normalization.
- *Step 2: Super-pixels* generation represents the initial step in super-pixel classification. In our experiments, we use the SLIC algorithm; which it has been exploited in many segmentation applications. However, SLIC depends on two essential parameters which are the compactness of super-pixels m and the number of super-pixels k.

  In order to find the right balance between the similarity of colors and super-pixel spatial proximity of the cytological images, we generate super-pixels by varying different constraints of $m = \{10;15;20\}$ and $k = \{100;500;1000\}$ as it is presented in Fig. 4.

Qualitatively, we estimate that the best compromise is obtained with $m = 20$ and $k = 500$, this values will be used to carry out our comparative experiments.

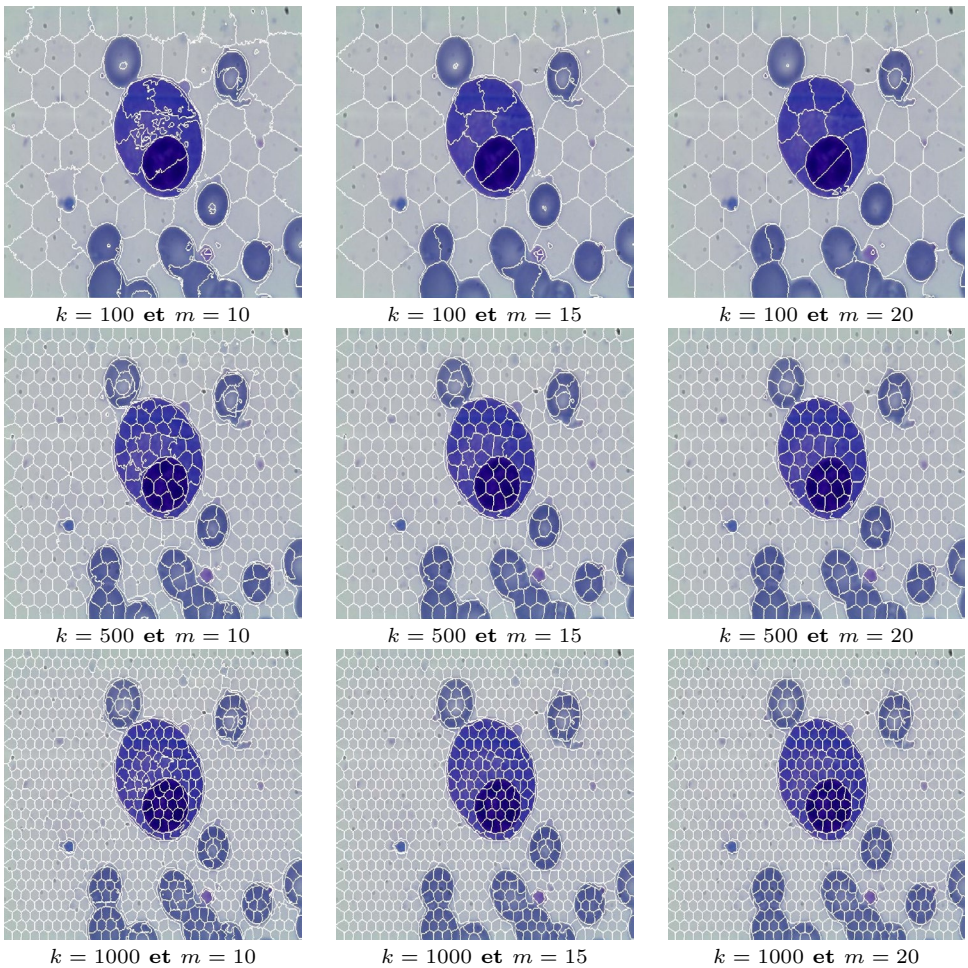

Fig. 4 Examples of super-pixels with the variation of constraints of m and k

– *Step 3: Color spaces* serves to treat each color space individually in the segmentation process.
– *Step 4: Features extraction* is a key step in the classification process; it involves studying different feature extraction techniques.
– *Step 5: Supervised classification* from step 4, the extracted data are presented to a supervised learning algorithm, to generate a classifier that will be exploited in the super-pixel classification. In this part, we use the SVM (Support Vector Machine) classifier with a Gaussian function and a non-linear separation, which is considered as a reference classifier for a variety of computer vision applications.

In the presented plan, three important steps achieve the objective of this study, color normalization (*Step 1*), the color space (*Step 2*) and super-pixel feature extraction (*step 4*).

Comparison protocol

Our proposal consists to manipulate 9 normalization processes, 4 color spaces and 4 feature extraction techniques (Table 2), making in all 144 possible combinations to analyze each treatment individually in the segmentation process. In fact, a combination is represented as follows:

$$N_i S_j F_k. \tag{14}$$

The Fig. 5 presents an experimentation example of CGWN normalization according to four color spaces and four feature extraction techniques.

Table 2 The codifications of each proposed combination

Normalization N		Color Spaces S		Feature extraction F	
i	Codification	j	Codification	k	Codification
$i = 1$	CGWN	$j = 1$	HSV	$k = 1$	Color mean (CM)
$i = 2$	CHROMA	$j = 2$	I1I2I3	$k = 2$	First-order statistics (FOS)
$i = 3$	CLAHE	$j = 3$	Lab	$k = 3$	Contrast
$i = 4$	GWN	$j = 4$	RGB	$k = 4$	Hu moments with intensity (Hu)
$i = 5$	HEQ				
$i = 6$	Lmax				
$i = 7$	MV				
$i = 8$	RGBcb				
$i = 9$	Without normalization (WN)				

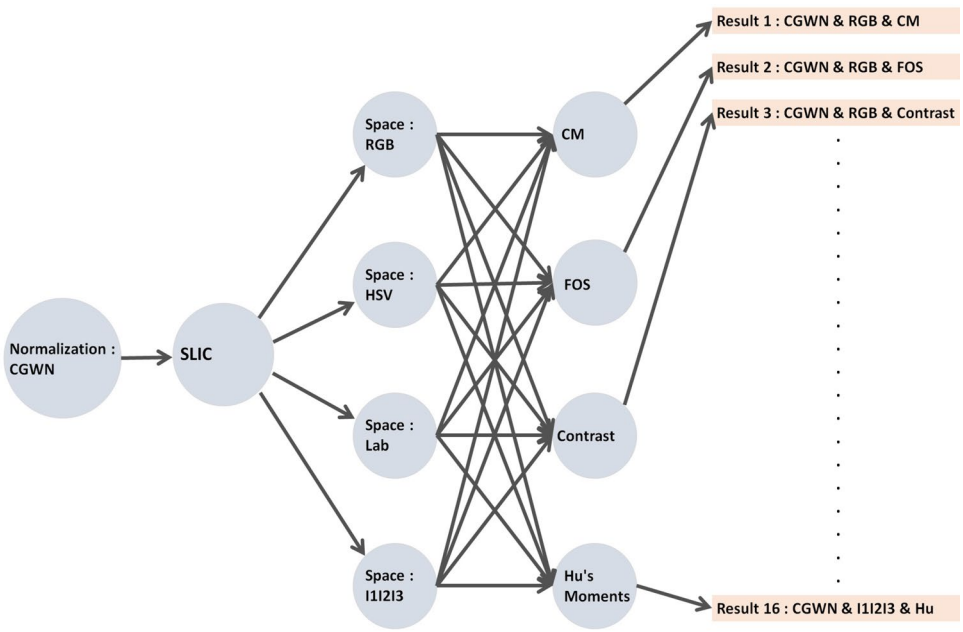

Fig. 5 Example of an experiment

In our experiments, we used the F-score measurement to discuss the obtained results. A high F-Score value indicates the relevance of the segmentation results. It is defined as follows:

$$F\text{-}score = 2\ \frac{Precision\ \cdot\ recall}{Precision + recall},$$

with:

$$Precision = \frac{TP}{TP + FP} \quad Recall = \frac{TP}{TP + FN}.$$

For a better results discussion, the Friedman test Post-Hoc proposed by Demsar [13] is applied. The Friedman non-parametric test is more adequate in order to detect whether statistically significant differences occur among examined methods over multiple application. The Post-hoc procedure of a multiple NxN comparison is an interesting tool, its main objective is to observe differences in performance, by making pair comparisons between each approach based on the $p - value$ calculation. A high $p - value$ means that the comparison results are similar, and a low $p - value$ means that

Table 3 Friedman ranking according to the *nucleus* segmentation with each N_i normalization

Average ranking									
Combination	N_1	N_2	N_3	N_4	N_5	N_6	N_7	N_8	N_9
S_1F_1	9.7414	13.1379	8.0172	11.4483	8.8448	13.5345	**3.2471**	13.908	13.6322
S_1F_2	**2.9425**	**4.2644**	**5.0862**	**4.6609**	9.023	**4.4598**	8.9425	10.5345	**4.6667**
S_1F_3	7.0977	9.2299	11.2126	11.4368	8.5977	11.7126	11.8966	6.1667	10.7874
S_1F_4	8.5172	14.6437	10.3103	10.8736	8.4195	10.7299	7.2471	10.6379	11.1897
S_2F_1	12.7126	**5.1207**	**5.6552**	9.8506	**8.0057**	7.1437	8.2529	7.3736	**5.8333**
S_2F_2	15.362	15.954	14.6839	15.3391	8.8218	15.2184	13.2069	8.1552	15.3391
S_2F_3	15.3621	11.4023	14.6379	15.3391	8.4828	15.2184	13.1897	**5.5345**	15.3391
S_2F_4	8.1667	**5.2759**	10.9253	**4.6667**	8.569	5.7356	**2.3276**	**3.6782**	**5.2184**
S_3F_1	11.023	9.2184	11.4253	5.8678	8.3161	6.5805	**2.9943**	13.3218	**5.9598**
S_3F_2	**3.546**	**4.908**	6.2759	**4.4253**	8.6724	6.6149	8.0057	**4.5805**	**5.9253**
S_3F_3	7.1609	9.2069	8.3391	8.0805	8.7644	9.408	12.4598	6.8161	8.8851
S_3F_4	10.2356	11.0575	**5.8448**	13.2644	**7.908**	8.8391	5.8333	**5.477**	12.2069
S_4F_1	**3.1207**	**3.6264**	**4.3161**	5.5575	**7.7356**	**5.3391**	8.5057	8.7529	**5.2356**
S_4F_2	**2.6839**	**3.2989**	6	5.2816	8.7471	**5.2816**	13.2069	15.1839	**5.2241**
S_4F_3	**4.6034**	**5.6494**	6.9828	**4.6437**	8.3908	**5.0517**	12.5517	6.1207	**5.2299**
S_4F_4	13.7241	10.0057	6.2874	5.2644	8.7011	**5.1322**	**4.1322**	9.7586	**5.3276**

Table 4 Friedman ranking according to the *cytoplasm* segmentation with each N_i normalization

Ranking									
Combination	N_1	N_2	N_3	N_4	N_5	N_6	N_7	N_8	N_9
S_1F_1	13.9253	13.9023	9.4253	14.3391	8.2644	14.5575	9.3391	13.2184	13.7011
S_1F_2	**2.908**	**2.6724**	5.5287	**3.5172**	8.7816	**2.7241**	8.6609	13.2184	**2.7241**
S_1F_3	6.1954	6.2874	7.6207	7.6379	9.1264	6.6264	6.7874	5.3276	6.7989
S_1F_4	9.6609	12.7356	10.2471	13.8046	7.6264	8.6897	10.1322	7.3793	11.0517
S_2F_1	8.8276	9.569	8.8218	10.0287	8.2011	10.3448	9.2931	6.9598	9.0517
S_2F_2	13.1379	14.2356	13.523	14.0287	9.5402	14.5345	10.6322	5.7069	14.046
S_2F_3	12.2586	14.2356	12.7126	9.2126	9.2874	14.454	6.5575	7.1437	13.8448
S_2F_4	12.2874	9.5172	7.2586	9.2069	7.431	6.7184	8.2874	6.4943	7.1897
S_3F_1	9.1839	8.7644	10.0172	7.046	8.0115	8.7759	9.3448	13.2184	9.2989
S_3F_2	**2.9138**	**3.3506**	**3.7356**	**2.9598**	8.3333	**2.8678**	8.4138	**2.9655**	**3.5172**
S_3F_3	5.6494	5.5115	7.3276	6.431	9.0747	5.6494	**4.523**	**4.3621**	6.3966
S_3F_4	11.8563	9.3851	10.954	12.7414	7.2069	11.2011	10.8276	7.5517	13.5862
S_4F_1	5.8851	6.477	7.9425	5.1207	8.5057	9.1322	9.454	7.7069	6.1839
S_4F_2	**2.0977**	**2.5862**	**4.8103**	**3.408**	8.7759	**3.3966**	10.4598	13.2184	**3.6954**
S_4F_3	5.2874	5.4598	6.9253	6.1667	9.2011	6.2471	7.8391	8.7759	6.0115
S_4F_4	13.9253	11.3103	9.1494	10.3506	8.6322	10.0805	**5.4483**	12.7529	8.9023

Table 5 Summary of the best combinations N_iF_k for each S_j color space

	Ranking	Rang1	Rang2	Rang3	Rang4	Rang5	Rang6
S_1	Nucleus	N_1F_2	N_2F_2	N_8F_3	–	–	–
	Cytoplasm	N_6F_2	N_9F_2	N_1F_2	N_2F_2	–	–
S_2	Nucleus	N_8F_4	N_2F_1	N_2F_4	N_8F_3	N_2F_2	N_4F_4
	Cytoplasm	N_2F_2	N_6F_4	–	–	–	–
S_3	Nucleus	N_8F_2	N_1F_2	N_2F_2	N_8F_4	N_4F_2	N_9F_2
	Cytoplasm	N_6F_2	N_1F_2	N_4F_2			–
S_4	Nucleus	N_1F_2	N_2F_2	N_1F_1	N_2F_1	–	–
	Cytoplasm	N_1F_2	N_2F_2	N_6F_2	–	–	–

Table 6 Synthesis of the best combinations N_iS_j for each F_k feature extraction technique

	Ranking	Rang1	Rang2	Rang3	Rang4	Rang5	Rang6
F_1	Nucleus	N_2S_4	N_1S_4	N_2S_2	–	–	–
	Cytoplasm	N_4S_4	N_4S_3	N_1S_4	N_2S_4	N_9S_4	–
F_2	Nucleus	N_1S_4	N_2S_4	N_8S_2	N_9S_4	N_6S_4	N_8S_1
	Cytoplasm	N_1S_4	N_6S_3	N_6S_4	–	–	–
F_3	Nucleus	N_1S_4	N_2S_4	N_8S_2	N_9S_4	N_6S_4	N_8S_1
	Cytoplasm	N_6S_3	N_1S_4	N_6S_4	–	–	–
F_4	Nucleus	N_8S_2	N_2S_2	N_8S_3	–	–	–
	Cytoplasm	N_6S_2	N_9S_2	N_6S_1	N_3S_2	–	–

the difference in results is significant. For more details, you can consult [13].

Results of normalization effect

For each N_i normalization, multiple comparisons were made using S_i and F_k to highlight the best performance of each normalization technique. Tables 3 and 4 show the average ranking of each N_i normalization according to S_j and F_k, the average ranking is calculated from the *F-score* results, the best rankings are displayed in bold. We observe that the best segmentation in N_1 is obtained by S_4F_2 combination ($AverageRanking = 2.6839$), and in N_2 by S_4F_2 combination($AverageRanking = 3.2989$). We make multiple comparisons between S_j and F_k for each normalization N_i to confirm the observations of the obtained ranking in the Tables 3 and 4.

Results of color effect

In this second part of our experiments, we complete our study with an analysis based on each S_j color space. We are mainly interested in analyzing the influence of the color information on the segmentation quality. All possible combinations between N_i normalization and F_k feature extraction are applied for each S_j color space separately to perform a non-parametric multiple comparison.

Table 7 Ranking of the best normalization techniques for the *nucleus* segmentation

Ranking	Comparison	*p*-value
1	$N_1S_4F_2$	–
2	$N_8S_2F_4$	0.677975
3	$N_2S_4F_2$	0.438286
4	$N_9S_1F_2$	0.000004
5	$N_6S_1F_2$	0.000001
6	$N_4S_3F_2$	0
7	$N_3S_4F_1$	0
8	$N_7S_2F_4$	0
9	$N_5S_4F_1$	0

The results of this analysis are summarized in Table 5, a ranking of the best combination for each S_j color space was highlighted. A second comparison is made taking into account only the ranking of the **Rang 1**, in order to identify the best color space S_j that can lead to a better super-pixel classification result.

Table 8 Ranking of the best normalization techniques for the *cytoplasm* segmentation

Ranking	Comparison	*p*-value
1	$N_1S_4F_2$	–
2	$N_6S_1F_2$	0.857206
3	$N_9S_1F_2$	0.846354
4	$N_2S_4F_2$	0.150022
5	$N_4S_3F_2$	0.008544
6	$N_8S_3F_2$	0
7	$N_3S_3F_2$	0
8	$N_7S_3F_3$	0
9	$N_5S_3F_4$	0

Table 9 Ranking of the best color spaces for the *nucleus* segmentation

Ranking	Comparison	*p*-value
1	$S_4N_1F_2$	–
2.5	$S_1N_1F_2$	0.481019
2.5	$S_2N_8F_4$	0.481019
4	$S_3N_8F_2$	0.00066

Results of feature extraction effect

Using the same protocol test, an analysis based on N_i normalization and S_j color space is performed for each F_k feature extraction technique separately. The analysis is summarized in Table 6.

Discussion

Analysis of normalization effect

Tables and show the statistical comparison of all normalization techniques. The Table 7 summarizes the statistical tests of the *nucleus* segmentation, N_1 normalization (CGWN) is ranked first as the best performing normalization for the *nucleus* segmentation, second as N_8 normalization (RGBcb) and third as N_2 normalization (CHROMA). A high measure of $p-value$ is observed for N_8 normalizations which means that N_1, N_8 normalizations can lead to similar results. The N_9 normalization is in the fourth position, it represents the performance of a segmentation **Without Normalization**, a large difference on performance ($p-value = 0.000004$) is observed compared to N_1 normalization. Based on these observations, it can be noted that the N_1 normalization has made considerable improvements in the segmentation of the *nucleus*.

Table 10 Ranking of the best color spaces for the *cytoplasm* segmentation

Ranking	Comparison	*p*-value
1	$S_4N_1F_2$	–
2	$S_1N_6F_2$	0.791588
3	$S_3N_6F_2$	0.037103
4	$S_2N_2F_2$	0

Table 11 Ranking of the best feature extraction technique for the *nucleus* segmentation

Ranking	Comparison	*p*-value
1	$F_2N_1S_4$	–
2	$F_4N_8S_2$	0.217515
3.5	$F_1N_2S_4$	0.000152
3.5	$F_3N_1S_4$	0.000152

Table 12 Ranking of the best feature extraction technique for the *cytoplasm* segmentation

Ranking	Comparison	*p*-value
1	$F_2N_1S_4$	–
2.5	$F_1N_4S_4$	0.013651
2.5	$F_3N_6S_3$	0.013651
4	$F_4N_6S_2$	0.002262

The non-parametric tests of the *cytoplasm* segmentation are displayed in Table 8. Similarly, the *cytoplasm* segmentation with N_1 normalization is ranked first. N_9 Normalization is ranked third which represents the performance of a segmentation **Without Normalization**. Therefore, we consider N_1 normalization as an interesting technique to improve the *nucleus* and *cytoplasm* segmentation results.

The non-parametric analysis shows that color normalization can influence the quality of segmentation. As a result, **CGWN** normalization is the most efficient technique, which will be exploited in the *nucleus* and *cytoplasm* segmentation.

Color analysis

The Friedman comparison is presented in Tables 9 and 10. In the *nucleus* segmentation (Table 9), the S_1 and S_2 color space (HSV and I1I2I3, respectively) give similar results, this is justified by the equality of $p-value$. In addition,

the S_3 space (Lab) has a significant performance variance compared to S_4 ($p - value = 0.00066$).

In the *cytoplasm* segmentation (Table 10), the comparison between the S_4 and S_1 spaces gives a $p - value = 0.79$, which means a strong similarity of performance. On the other hand, the S_3 and S_2 spaces show an important difference performance compared to S_4.

It is concluded that the S_4 space (RGB) is ranked first as the most efficient space in the *nucleus* and the *cytoplasm* segmentation, and the S_1 space (HSV) is ranked second.

Feature extraction analysis

Subsequently, we are interested in our study to the results of **Rang 1** in Table 6. A second non-parametric analysis is performed to compare feature extraction techniques. Tables 11 and 12 show the $p - value$ statistics in comparison with the best performing feature extraction technique.

In the *nucleus* segmentation (Table 11), the F_2 feature extraction of the FOS technique is classified in the first position, the second position is for the F_4 feature extraction (Hu) with a difference performance $p - value = 0.21$, after F_1 and F_3 are ranked last with a significant performance variance ($p - value = 0.000152$).

In the *cytoplasm* segmentation (Table 12), we also observed that F_2 Feature extraction (FOS) is the most reliable technique to obtain a good *cytoplasm* segmentation, the F_1 (CM) and F_3 (contrast) Feature extraction obtained the same ranking with a significant performance variance ($p - value = 0.013$) compared to F_2, and the F_4 feature extraction (Hu) is ranked last.

Synthesis of experiments

The conducted experiments are based essentially on three analysis topics: color normalization, space color and superpixel feature extraction. Through non-parametric tests ($p - value$), we made the multiple comparisons between all possible combinations of $N_iS_jF_k$, with $i = 9$, $j = 4$ and $k = 4$. The results allowed us to select the best $N_iS_jF_k$ combinations, which give the best measures of *F-score* in segmentation (Table 13). In Table 14, the statistical results demonstrate that $N_1S_4F_2$ is the most reliable combination that can be exploited in the *nucleus* and *cytoplasm* segmentation, i.e. **CGWN** normalization, **RGB** color space and **FOS** feature extraction. Figure 6 shows the segmentation results using $N_1S_4F_2$ combination, as is shown the *nucleus* and *cytoplasm* segmentation are perfectly segmented in comparison by the expert segmentation. We also display the *F-score* results for each image in Fig. 6. We observe that the obtained segmentation is of better quality which is confirmed by *F-score*.

A Github repository with additional materials and the complete comparison results can be found at this link: https

Table 13 Synthesis of the best combinations $N_iS_jF_k$ for the *nucleus* and *cytoplasm* segmentation

Ranking	Normalization		Color		Feature extraction	
	Nucleus	*Cytoplasm*	*Nucleus*	*Cytoplasm*	*Nucleus*	*Cytoplasm*
Rang1	$N_1S_4F_2$	$N_1S_4F_2$	$N_1S_4F_2$	$N_1S_4F_2$	$N_1S_4F_2$	$N_1S_4F_2$
Rang2	$N_8S_2F_4$	$N_6S_1F_2$	$N_1S_1F_2$	$N_6S_1F_2$	$N_8S_2F_4$	$N_4S_4F_1$
Rang3	$N_2S_4F_2$	$N_9S_1F_2$	$N_8S_2F_4$	$N_6S_3F_2$	$N_2S_4F_1$	$N_6S_3F_3$
Rang4	$N_9S_1F_2$	$N_2S_4F_2$	$N_8S_3F_2$	$N_2S_2F_2$	$N_1S_4F_3$	$N_6S_2F_4$
Rang5	$N_6S_1F_2$	$N_4S_3F_2$	–	–	–	–
Rang6	$N_4S_3F_2$	$N_8S_3F_2$	–	–	–	–
Rang7	$N_3S_4F_1$	$N_3S_3F_2$	–	–	–	–
Rang8	$N_7S_2F_4$	$N_7S_3F_3$	–	–	–	–
Rang9	$N_5S_4F_1$	$N_5S_3F_4$	–	–	–	–

Table 14 Ranking of the best normalization, color spaces and feature extraction techniques for the *nucleus* and *cytoplasm* segmentation

	Ranking	Combination	*p*-value	Normalization	Color spaces	Feature extraction
Nucleus	1	$N_1S_4F_2$	–	CGWN	RGB	FOS
	2	$N_1S_1F_2$	0.518317	CGWN	HSV	FOS
	3	$N_8S_2F_4$	0.347447	RGBcb	I1I2I3	Hu
	4	$N_2S_4F_1$	0.022012	CHROMA	RGB	CM
Cytoplasm	1	$N_1S_4F_2$	–	CGWN	RGB	FOS
	2	$N_6S_1F_2$	0.883286	Lmax	HSV	FOS
	3	$N_1S_4F_1$	0.000001	CGWN	RGB	CM
	4	$N_1S_3F_3$	0	CGWN	Lab	Contrast

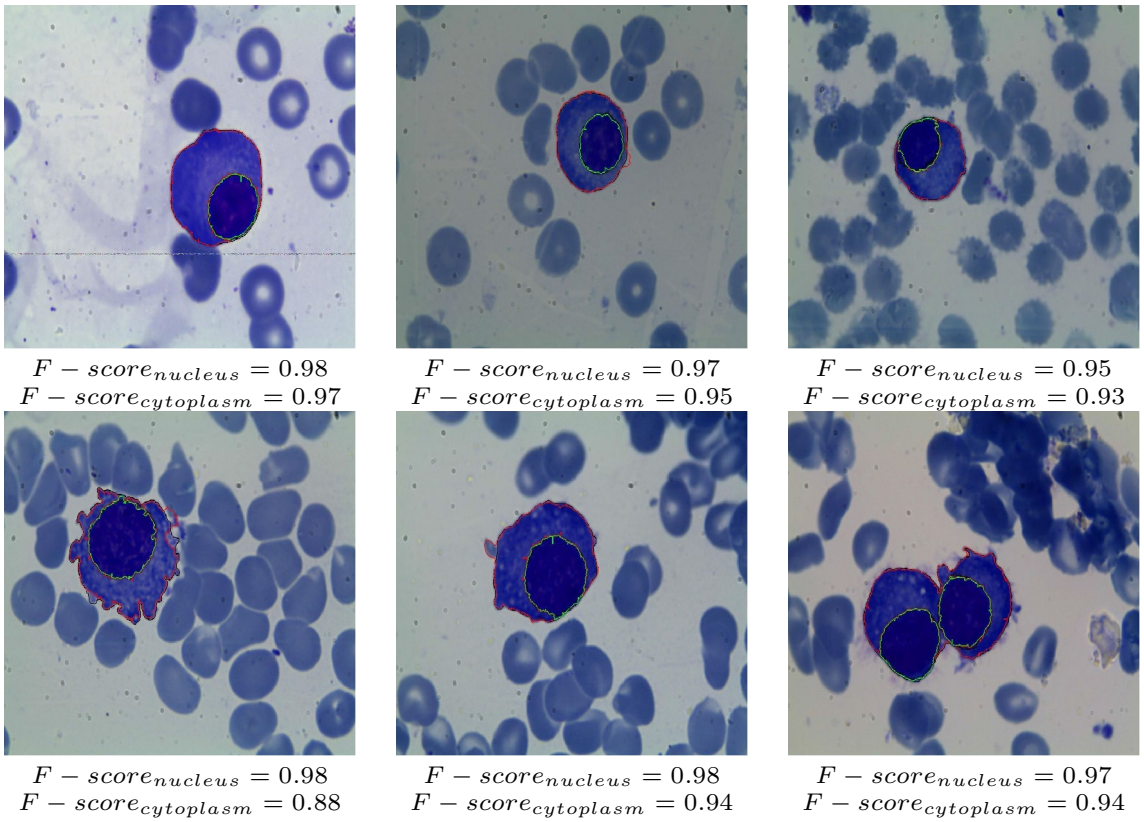

Fig. 6 Segmentation by super-pixel classification. The *nucleus* is segmented by a green outline, the *cytoplasm* is segmented by a red outline, and the segmentation of the expert is given by a black outline

://github.com/Mostafa-EHD/Super-Pixel-Classification-Cyto-images.git

Conclusion

In this paper, we conducted multiple experiments to allow a careful analysis of the super-pixel classification concept, in applying the segmentation of cytological images and automatic recognition of white blood cells. The key idea of this study was performed on the quality of the super-pixel feature extraction, exploiting the color component information. Therefore, color normalization, color component and super-pixel feature extraction were the main topics of this work.

Does the color normalization have an influence on the segmentation? It is the first question which has been treated in this study. From the results obtained, we answer by *"YES"*. Eight normalization techniques were analyzed in comparison with the results without normalization, and normalization with **CGWN** showed positive influence on the *nucleus* and *cytoplasm* segmentation.

Which is the best color space? Obviously the choice of the color space is an important question, to do this, we analyzed four most relevant color spaces. Based on a non-parametric analysis, we obtained that the source space of **RGB** is the color space which gives the best segmentation performance.

What is the best mode of feature extraction? The reliability of super-pixel classification lies in the reliability of the super-pixel feature extraction. Based on our experiments, from four feature extraction techniques, the **FOS** gives us segmentation results that are very close to the segmentation of the expert. What makes the **FOS** the most reliable mode that allows to represent the super-pixel classification.

The statistical comparisons made allowed us to justify the choice of the relevant feature extraction, in order to take into account the information present in the super-pixels.

Future works are currently underway, where we try to answer to the question *which is the best techniques for intensity texture features that gives an efficient description of the super-pixels texture?*. Thereby, we are working on the application of texture analysis which is an important part of many computer image analysis applications for image classification or to study the local spatial variations

in gray level intensity for segmentation task. Its ability to characterize the visual homogeneity of a given area of an image allows a texture analysis that takes into account both spatial and spectral aspects. Therefore, we will deepen our study by the application of intensity texture features as: second order statistical, wavelet features, Gabor Filter, Fractal texture features, etc.

Funding No funding was received.

Compliance with ethical standards

Conflict of interest The authors declare that they have no conflict of interest.

Ethical approval This article does not contain any studies with human participants or animals performed by any of the authors.

Informed consent Not applicable.

References

1. Abu-Mostafa YS, Psaltis D (1984) Recognitive aspects of moment invariants. IEEE Trans Pattern Anal Mach Intell 6:698–706
2. Achanta R, Shaji A, Smith K, Lucchi A, Fua P, Süsstrunk S (2012) Slic superpixels compared to state-of-the-art superpixel methods. IEEE Trans Pattern Anal Mach Intell 34(11):2274–2282
3. Alata O, Burie JC, Moussa A, Fernandez-Maloigne C (2011) Choice of a pertinent color space for color texture characterization using parametric spectral analysis. Pattern Recognit 44(1):16–31
4. Artan Y (2011) Interactive image segmentation using machine learning techniques. In: 2011 Canadian conference on computer and robot vision, pp 264–269. https://doi.org/10.1109/CRV.2011.42
5. Bechar MEA, Settouti N, Barra V, Chikh MA (2018) Semi-supervised superpixel classification for medical images segmentation: application to detection of glaucoma disease. Multidimens Syst Signal Process 29(3):979–998. https://doi.org/10.1007/s11045-017-0483-y
6. Benazzouz M, Baghli I, Chikh MA (2013) Microscopic image segmentation based on pixel classification and dimensionality reduction. Int J Imaging Syst Technol 23(1):22–28. http://dblp.uni-trier.de/db/journals/imst/imst23.html#BenazzouzBC13
7. Borovec J, Svihlík J, Kybic J, Habart D (2017) Supervised and unsupervised segmentation using superpixels, model estimation, and graph cut. J Electron Imaging 26(6):61610
8. Boschetto D, Grisan E (2017) Superpixel-based classification of gastric chromoendoscopy images. In: Medical imaging: computer-aided diagnosis, SPIE, SPIE Proceedings, vol 10134, p 101340W
9. Boyce JF, Hossack W (1983) Moment invariants for pattern recognition. Pattern Recognit Lett 1(5–6):451–456
10. Cernadas E, Fernández-Delgado M, González-Rufino E, Carrión P (2017) Influence of normalization and color space to color texture classification. Pattern Recognit 61:120–138
11. Cheng L, Ye N, Yu W, Cheah A (2011) Discriminative segmentation of microscopic cellular images. In: International conference on medical image computing and computer-assisted intervention. Springer, New York, pp 637–644
12. Choi JY, Ro YM, Plataniotis KN (2012) Color local texture features for color face recognition. IEEE Trans Image Process 21(3):1366–1380
13. Demsar J (2006) Statistical comparisons of classifiers over multiple data sets. J Mach Learn Res 7:1–30. http://dl.acm.org/citation.cfm?id=1248547.1248548
14. Drimbarean A, Whelan PF (2001) Experiments in colour texture analysis. Pattern Recognit Lett 22(10):1161–1167
15. Ebner M (2007) Color constancy, vol 6. Wiley, New York
16. Finlayson GD, Schiele B, Crowley JL (1998) Comprehensive colour image normalization. In: European conference on computer vision. Springer, New York, pp 475–490
17. Forsythe J, Kurlin V (2017) Convex constrained meshes for superpixel segmentations of images. J Electron Imaging 26(6):61609
18. Fulkerson B, Vedaldi A, Soatto S et al (2009) Class segmentation and object localization with superpixel neighborhoods. In: ICCV, Citeseer, vol 9, pp 670–677
19. González-Rufino E, Carrión P, Cernadas E, Fernández-Delgado M, Domínguez-Petit R (2013) Exhaustive comparison of colour texture features and classification methods to discriminate cells categories in histological images of fish ovary. Pattern Recogn 46(9):2391–2407
20. Gu L, Zheng Y, Bise R, Sato I, Imanishi N, Aiso S (2017) Semi-supervised learning for biomedical image segmentation via forest oriented super pixels(voxels). In: MICCAI
21. He X, Zemel RS, Ray D (2006) Learning and incorporating top-down cues in image segmentation. In: European conference on computer vision. Springer, New York, pp 338–351
22. Hoiem D, Efros AA, Hebert M (2005) Automatic photo pop-up. ACM Trans Graph 24(3):577–584
23. Hu MK (1962) Visual pattern recognition by moment invariants. IRE Trans Inf Theory 8(2):179–187
24. Irshad H, Veillard A, Roux L, Racoceanu D (2014) Methods for nuclei detection, segmentation, and classification in digital histopathology: a review-current status and future potential. IEEE Rev Biomed Eng 7:97–114
25. Kakumanu P, Makrogiannis S, Bourbakis N (2007) A survey of skin-color modeling and detection methods. Pattern Recognit 40(3):1106–1122
26. Kandaswamy U, Schuckers SA, Adjeroh D (2011) Comparison of texture analysis schemes under nonideal conditions. IEEE Trans Image Process 20(8):2260–2275
27. Kandaswamy U, Adjeroh DA, Schuckers S, Hanbury A (2012) Robust color texture features under varying illumination conditions. IEEE Trans Syst Man Cybern Part B 42(1):58–68
28. Levinshtein A, Dickinson SJ, Sminchisescu C (2009) Multiscale symmetric part detection and grouping. In: ICCV, pp 2162–2169
29. Li Y, Sun J, Tang CK, Shum HY (2004) Lazy snapping. In: ACM transactions on graphics (ToG), vol 23. ACM, New York, pp 303–308
30. Limare N, Lisani JL, Morel JM, Petro AB, Sbert C (2011) Simplest color balance. Image Process Line 1:297–315
31. Mäenpää T, Pietikäinen M (2004) Classification with color and texture: jointly or separately? Pattern Recognit 37(8):1629–1640
32. Magaña-Tellez O, Vrigkas M, Nikou C, Kakadiaris IA (2018) SPICE: superpixel classification for cell detection and counting. In: VISIGRAPP (4: VISAPP). SciTePress, pp 485–490
33. Mery D, Filbert D (2002) Classification of potential defects in automated inspection of aluminium castings using statistical pattern recognition. In: Proceedings of 8th European conference on non-destructive testing (ECNDT 2002), pp 17–21
34. Nakamura K, Hong B (2017) Hierarchical image segmentation via recursive superpixel with adaptive regularity. J Electron Imaging 26(6):61602
35. Nava R, Kybic J (2015) Supertexton-based segmentation in early drosophila oogenesis. In: ICIP. IEEE, pp 2656–2659

36. Paschos G (2001) Perceptually uniform color spaces for color texture analysis: an empirical evaluation. IEEE Trans Image Process 10(6):932–937
37. Ren X, Malik J (2003a) Learning a classification model for segmentation. In: Computer vision. Proceedings. Ninth IEEE international conference on. IEEE, pp 10–17
38. Ren X, Malik J (2003b) Learning a classification model for segmentation. IEEE, p 10
39. Schaefer G, Finlayson G, Hordley S, Tian G (2005) Illuminant and device invariant color using histogram equalization. Pattern Recognit 28:179–190
40. Vandenbroucke N, Macaire L, Postaire JG (2003) Color image segmentation by pixel classification in an adapted hybrid color space. application to soccer image analysis. Comput Vision Image Underst 90(2):190–216
41. Vandenbroucke N, Busin L, Macaire L (2015) Unsupervised color-image segmentation by multicolor space iterative pixel classification. J Electron Imaging 24(2):023032–023032
42. Varma M, Zisserman A (2005) A statistical approach to texture classification from single images. Int J Comput Vis 62(1):61–81
43. Varma M, Zisserman A (2009) A statistical approach to material classification using image patch exemplars. IEEE Trans Pattern Anal Mach Intell 31(11):2032–2047
44. Wu W, Chen AY, Zhao L, Corso JJ (2014) Brain tumor detection and segmentation in a crf (conditional random fields) framework with pixel-pairwise affinity and superpixel-level features. Int J Comput Assist Radiol Surg 9(2):241–253
45. Xu J, Ishikawa H, Wollstein G, Schuman JS (2011) 3d optical coherence tomography super pixel with machine classifier analysis for glaucoma detection. In: EMBC. IEEE, pp 3395–3398
46. Zuiderveld K (1994) Contrast limited adaptive histogram equalization. In: Graphics gems IV. Academic Press Professional, Inc., New York, pp 474–485